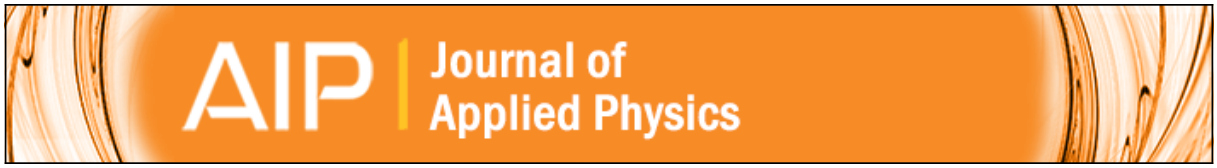


# Effect of Al substitution on the local environments and magnetic properties of partially nitrogenated (Er 0.5 Pr 0.5 ) 2 Fe 17 permanent magnets

V. G. Harris, D. J. Fatemi, K. G. Suresh, and K. V. S. Rama Rao

Citation: Journal of Applied Physics **83**, 6920 (1998); doi: 10.1063/1.367711
View online: http://dx.doi.org/10.1063/1.367711
View Table of Contents: http://scitation.aip.org/content/aip/journal/jap/83/11?ver=pdfcov
Published by the AIP Publishing

**Articles you may be interested in**

Realization of small intrinsic hysteresis with large magnetic entropy change in La0.8Pr0.2(Fe0.88Si0.10Al0.02)13 by controlling itinerant-electron characteristics
Appl. Phys. Lett. **104**, 122410 (2014); 10.1063/1.4869957

Effect of Al on the magnetic properties of Pr 3 ( Fe 1 − x Al x ) 27.5 Ti 1.5 ( x = 0.1 , 0.2, and 0.3)
J. Appl. Phys. **99**, 08P301 (2006); 10.1063/1.2167052

Structural and magnetic properties of ( Sm , Pr ) 3 ( Fe 1 − x Al x ) 27.5 Ti 1.5 [ x = 0.1 , 0.2 , 0.3 ]
J. Appl. Phys. **97**, 10H105 (2005); 10.1063/1.1851880

Effect of Mn substitution on the volume and magnetic properties of Er 2 Fe 17
J. Appl. Phys. **92**, 1453 (2002); 10.1063/1.1489718

Thermal expansion anomaly of Pr 2 AlFe 13 Mn 3 compound near its Curie temperature and magnetic properties of Pr 2 AlFe 16−x Mn x compounds
J. Appl. Phys. **91**, 8219 (2002); 10.1063/1.1447515


[This article is copyrighted as indicated in the article. Reuse of AIP content is subject to the terms at: http://scitation.aip.org/termsconditions. Downloaded to ] IP: 131.193.242.169 On: Thu, 27 Nov 2014 05:08:12

# Effect of Al substitution on the local environments and magnetic properties of partially nitrogenated $(Er_{0.5}Pr_{0.5})_2Fe_{17}$ permanent magnets

V. G. Harris and D. J. Fatemi
*U.S. Naval Research Laboratory, Washington, D.C. 20375*

K. G. Suresh and K. V. S. Rama Rao
*Department of Physics, Indian Institute of Technology, Madras-600 036, India*

Extended x-ray absorption fine structure measurements of the Fe K, and Pr and Er $L_{III}$ absorption edges, were carried out to elucidate the relationship between the local structure and magnetism in Al substituted, partially nitrogenated $(Er_{0.5}Pr_{0.5})_2Fe_{17}$ permanent magnets. We find that the nitrogenation acts to dilate both the Fe–Fe and the (Pr,Er)–Fe bonds, thus raising the $T_C$ via a magnetovolume effect. However, nitrogenation of Al-substituted samples acts to decrease the average Fe–Fe bond distance, thus reducing the exchange on the Fe sublattice and lowering $T_C$ relative to the nitrogenated parent compound. This is opposite to the trend measured in systems when N is absent. © *1998 American Institute of Physics.* [S0021-8979(98)36011-9]

## I. INTRODUCTION

In recent years the magnetovolume enhancement of the magnetic properties in the $R_2T_{17}$ (R: rare earths) permanent magnet compounds has been the subject of much activity. This trend has been spurred largely by the discovery that nitrogenation of these compounds expands the transition metal sublattice and results in a significant increase in the Curie temperature $(T_C)$.[1–3] Following in this vein, others have experimented with the substitution of Al and Ga with mixed results.[4–8] For example, combining neutron diffraction (ND) and Mossbauer effect (ME) measurements, Long *et al.*[4] and Yelon *et al.*[5] have reported compressive studies of the structure and magnetic properties of Al substituted $Nd_2Fe_{17}$. This group of researchers have also reported similar styled investigations of the effects of nitrogenation on $Nd_2Fe_{17}$[9] and $Pr_2Fe_{17}$,[10] and the effects of Ga substitution in the $Nd_2Fe_{17}$ system.[6] Suresh and Rama Rao (SRR) have reported on the magnetic, structural and transport properties of the $(Er_yPr_{1-y})_2Fe_{17}$ compounds,[11,12] as well as the effects of Al substitution,[8] nitrogenation,[12] and the combined use of Al substitution and nitrogenation on these properties.[7,13]

In the case of $Nd_2Fe_{17-x}Al_x$, Long and Yelon report a near-linear increase in lattice parameters and unit cell volumes with increasing $x$. A similar result was found by Suresh and Rama Rao in the $(Er_yPr_{1-y})_2Fe_{17-x}Al_x$ system. The $T_C$ is reported to increase with increasing Al content for the $Nd_2Fe_{17-x}Al_x$ samples, reaching a maximum near $x=3.5$. For the $(Er_yPr_{1-y})_2Fe_{17-x}Al_x$ samples, $T_C$ reaches a maximum for $x=3$, then drops precipitously for $x>4$. The agreement between these results and those of Long *et al.*[4,9,10] and Yelon *et al.*[5] suggest that the choice of $R$ plays a minor role in the effect of both Al substitution and nitrogenation.

When Al substitution and nitrogenation are used in conjunction these trends appear to be violated. Taking the case of $(Er_{0.5}Pr_{0.5})_2Fe_{17-x}Al_xN_y$, where $y=1$ and $x=0-5$, $T_C$ decreases from the nitrided parent compound with increasing $x$, ultimately having no effect on the $T_C$ for $x>4$. This result appears to be closely related to the degree of nitrogenation achievable when the parent compound contains Al substituted for Fe. Suresh and Rama Rao report, in agreement with Buschow *et al.*, the amount of nitrogen one can incorporate into the 2:17 structure is inversely proportional to the amount of Al, with $y$ decreasing with increasing $x$ until $y=0$ for $x=6$.[7]

In this article, we explore the effects of Al substitution on the local structure and magnetism of the permanent magnet, $(Er_{0.5}Pr_{0.5})_2Fe_{17-x}Al_xN_y$.

## II. EXPERIMENT

The compounds were prepared by arc melting elements of 99.9% purity for Pr and Er and 99.99% purity for Fe and Al under dynamic positive pressure of Ar gas. The melted ingots were then homogenized at 900 °C for 7 days. The nitrogenation was carried out using a high pressure apparatus that was specifically designed for this purpose. The degree of nitrogenation was measured by monitoring the pressure drop in the reactor due to absorption by the sample. This apparatus is described in detail in Ref. 12.

Powder x-ray diffraction, using a fixed anode Co target, verified that all samples were nearly pure phase, with some having trace amounts of $\alpha$-Fe. For the range of Al substitution that we study here, $0 \leqslant x \leqslant 3$, the $a$ and $c$ parameters are measured to increase ~1%.

Magnetization measurements were carried out using a PAR vibrating sample magnetometer in the temperature range of 28–800 K, and Mossbauer effect (ME) measurements using a conventional fixed acceleration spectrometer with a 20 mCi $^{57}$Co source embedded in a Rh matrix over a temperature range of 18–700 K. We direct the reader to Refs. 7 and 13 for details of the long-range-structure and magnetic properties of these samples.

In preparation of x-ray absorption measurements the powder samples were spread onto 3M Scotch Magic Tape™. Multiple layers of these powdered tapes were stacked in order to tailor the amount of absorption by the sample at the absorption edge being measured. This was done so as to optimize the signal to noise and to improve the uniformity of the sample exposed to the radiation. The x-ray absorption coefficient, in the range of the Fe K and Pr and Er $L_{III}$ ab-

 © 1998 American Institute of Physics

[This article is copyrighted as indicated in the article. Reuse of AIP content is subject to the terms at: http://scitation.aip.org/termsconditions. Downloaded to ] IP: 131.193.242.169 On: Thu, 27 Nov 2014 05:08:12

sorption edges, were measured in transmission mode using the X23B beamline[14] at the National Synchrotron Light Source (Brookhaven National Laboratory).

Following the procedural steps outlined in Ref. 15, the extended fine structure above the absorption edge was isolated, normalized to the edge energy and step height, and converted to photoelectron wave vector space ($k$). In $k$ space, a cubic spline background was fit and removed from the data to minimize the nonoscillatory atomic background curvature. these data were then Fourier transformed (FT) to radial coordinates for examination of the local environments around the absorbing atoms. In this form the FT peaks are offset from their true bond distances by an electronic phase shift.

Quantitative analysis of the local environment around Fe, Pr, and Er was performed by Fourier-filtering the NN peak in the FT EXAFS spectra and least squares fitting these data with simulated single-scattering EXAFS data generated using the FEFF (vs 6) codes of Rehr *et al.*[16] This type analysis provides a quantitative measure of the nearest neighbor (NN) distance (i.e., bond lengths), Debye–Waller coefficients (DWCs) (i.e., thermal and static atomic disorder), and the coordination number, i.e., the total number of atoms contributing to the local coordination sphere around the absorbing atoms.

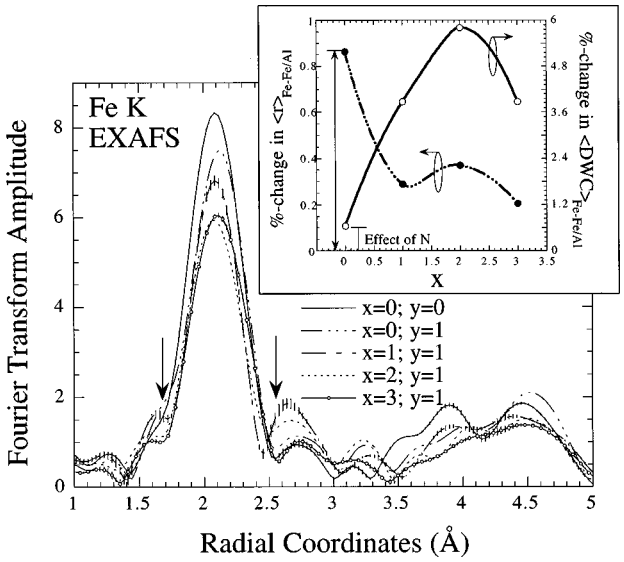


FIG. 1. Fourier transformed Fe K EXAFS for $(Er_{0.5}Pr_{0.5})_2Fe_{17-x}Al_xN_y$ where $x=0$, 1, 2 and 3 and $y=0$, 1. A $k^3$-weighting was applied to a $k$-range of 2.3–13.25 Å$^{-1}$. The inset panel depicts a plot of the percent change in the calculated average Fe–Fe/Al bond distance and the Debye–Waller coefficient for the Fe coordination sphere relative to the same in the parent compound. These data were deduced from a least-squares fitting of a FF $r$ range indicated by the arrows.

## III. RESULTS AND DISCUSSION

We are limited by space considerations and provide only EXAFS analysis of the Fe K and Pr $L_{III}$ EXAFS. The Er $L_{III}$ analysis is omitted here and will be presented elsewhere.

Figure 1 is a plot of the FT Fe EXAFS collected from the Al-substituted and nitrided samples, together with data for the parent compound. These data have been analyzed using identical background removal procedures and FT parameters, and are plotted on the same axes to allow for direct comparison. The $x$ axis is limited to 1.0 Å $<r<$5.0 Å to allow a clear inspection of the NN region. Samples having $x=0$, $y=1$; $x=0$, $y=0$; and $x=3$, $y=1$; are plotted with error bars that were calculated to reflect both the statistical uncertainty and the error introduced to the data from the procedural steps prior to and including the Fourier transformation. The inset panel depicts a plot of the average Fe–Fe/Al bond distance (henceforth denoted $\langle r\rangle_{\text{Fe–Fe/Al}}$ and the average Fe–Fe/Al DWC (henceforth denoted $\langle \text{DWC}\rangle_{\text{Fe–Fe/Al}}$) calculated for the atoms contributing to the NN peak as a function of $x$. Values coinciding to the parent compound are to provide a reference baseline.

In the FT data of Fig. 1 we see that significant structural change occurs around the Fe atoms with the substitution of Al. These are most visible as changes in the Fourier peak amplitudes appearing over 2 Å$<r<$5 Å and a shift in the position of the NN Peak. Because the NN peak of Fe is dominated by other Fe and Al atoms that are distributed on 4 inequivalent sites (i.e., $6c$, $9d$,$18f$,$18h$) we opt to describe the environment as an average Fe–Fe/Al bond unless otherwise specified. This simplification reduces the number of adjustable parameters in our fitting analysis from as many as 12 to no more than 3.

Upon nitrogenation the $\langle r\rangle_{\text{Fe–Fe/Al}}$ increases 0.9% from that of the parent compound. This result is a direct measurement of the dilation of the Fe coordination sphere which reflects the expansion of the Fe sublattice and accounts for the widely reported increase in Curie temperature experienced when the 2:17$s$ are nitrided. With the substitution of Al we observe that $\langle r\rangle_{\text{Fe–Fe/Al}}$ decreases abruptly ($-0.6\%$), plateaus, and then continues its decrease. Although, others have reported a unit cell volume increase with the substitution of small amounts of Al ($x<4$) (sans N),[4,8] we observe that in partially nitrided samples, the Al acts to contract the Fe coordination sphere relative to the nitrided baseline. This contraction is no doubt responsible for the measured decrease in Curie temperature in these compounds, and is consistent with the ME results of Suresh and Rama Rao[13] who found that the $T_C$ and the HFF of all Fe sites reduce with increased Al content for these samples.

The $\langle \text{DWC}\rangle_{\text{Fe–Fe/Al}}$ increases with increased Al content for $0<x<2$, and experiences a relative decrease for $x=3$. Because it is reasonable for one to assume that the thermal component to the DWC does not change appreciably with $x$, this trend largely reflects the static displacements of atoms about their mean bond distance. The abrupt reversal in the DWC for $x=3$, and the corresponding reduction in the $\langle r\rangle_{\text{Fe–Fe/Al}}$, signals increased ordering and a closer packing of atoms around the Fe atoms for $x=3$.

In separate fitting analyses, the Fe–Al correlations were fit simultaneously with the Fe–Fe correlations in the same manner as described in Sec. II B. These fitting results (not shown) indicate that the Fe–Al bond undergoes an abrupt decrease for $x=3$. The most plausible explanation of this result and the behavior of the average Fe environment is a

[This article is copyrighted as indicated in the article. Reuse of AIP content is subject to the terms at: http://scitation.aip.org/termsconditions. Downloaded to ] IP: 131.193.242.169 On: Thu, 27 Nov 2014 05:08:12

redistribution of Al atoms to sites having a closer NN distance.

Long *et al.*[4] report that Al atoms preferentially reside in the 18*h* site for low $x$ (i.e., $x<4$), and prefer the 6*c* and 18*f* sites for higher $x$ (i.e., $x>6$). Because the 18*h* sites have a NN distance of ~2.576 Å, while the 6*c* sites have a longer average NN distance of ~2.675 Å, one would expect a slight dilation of the Fe coordination sphere.[17] Instead we measure a distinct contraction of the Fe coordination sphere, suggesting that the behavior of the Al site filling is significantly effected by the presence of the N ions. Our measured contraction is more consistent with a redistribution of Al atoms to the 9*d* sites although we cannot rule out some other electronic interaction which might facilitate a contracted bond distance without the need for redistribution of sites.

Figure 2 is plots of FT Pr $L_{III}$ EXAFS data for all samples. Because of the onset of the Fe K transition at 7112 eV, the Pr $L_{III}$ extended fine structure is terminated at approximately 11 $Å^{-1}$. Data for samples $x=0$, $y=0$; $x=0$, $y=1$; and $x=3$, $y=1$ are plotted with error bars. Like the Fe data of Fig. 1, we see that nitrogenation acts to increase the radius of the Pr coordination sphere by 1.7%. The $\langle DWC\rangle_{Pr-Fe/Al}$ increases 24%, compared to the modest increases of <1% for the Fe environment. This effect is fully consistent with what one would expect if the N ions were to occupy sites in close proximity to the *R* sites creating static strain fields between the R and Fe/Al NN atoms. This observation is consistent with the results of Capehart, Mishra, and Pinkerton who performed EXAFS studies to determine the site occupation of the N interstitials, and concluded that they reside on the 9*e* sites.[18]

With Al substitution, the Pr environment experiences a steady increase in the atomic disorder as evidenced by the increase in $\langle DWC\rangle_{Pr-Fe/Al}$. In addition, the $\langle r\rangle_{Pr-Fe/Al}$ increases 1.0% for the range $1<x<3$, then experiences a small dip for $x=3$. However, the FT of the $x=3$ data clearly shows a large asymmetry in the NN environment indicating at least a bimodal distribution of bonds. Because we fit this range of data with a single ''average'' bond length a physical interpretation of the fitting results may not be tenable. Alternatively, the appearance of this high-*r* asymmetry in the NN region is consistent with a preferential filling of Al on the 9*d* sites which have the largest Pr–Fe/Al bond distance, 3.342 Å. This result alone would not be compelling save for the trend in the Fe EXAFS data which supports a redistribution of Al atoms to the 9*d* sites as a source of the measured contraction of the Fe coordination sphere.

In summary, we find the act of nitriding the $(Er_{0.5}Pr_{0.5})_2Fe_{17}$ structure is to dilate both the Fe and Pr coordination spheres leading to an increase in the $T_C$ via a positive magnetovolume effect on the Fe sublattice. Second, we report that in the concurrent use of Al substitution and partial nitrogenation acts to reduce the radius of the Fe coordination sphere thus reducing the Fe–Fe exchange and lowering $T_C$.

We observe local structural changes around Fe and Pr with Al substitution that suggest either a preferential redistribution of Al atoms to the 9*d* sites for $x\geqslant 3$, or an electronic interaction that facilitates a contracted bonding arrangement for Fe and a dilated bonding arrangement for Pr. This result suggest that the presence of N in the unit cell alters the site filling characteristics of Al in this compound.

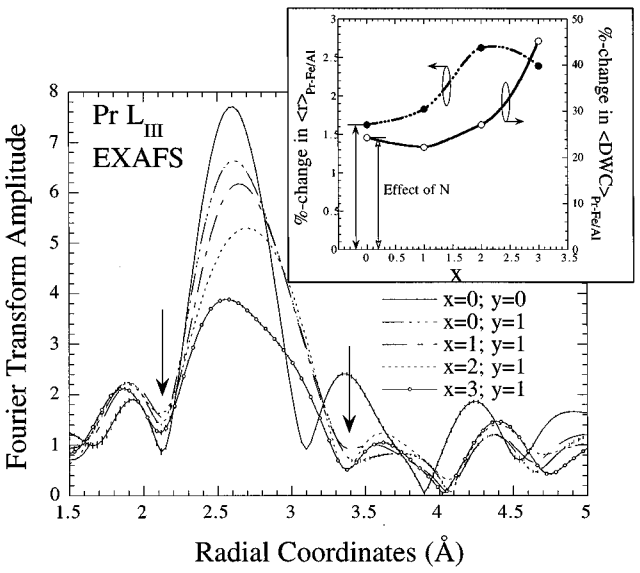


FIG. 2. Fourier transformed Pr $L_{III}$ EXAFS for $(Er_{0.5}Pr_{0.5})_2Fe_{17-x}Al_xN_y$, where $x=0,1,2$ and 3 and $y=0$, 1. A $k^3$-weighting was applied to a $k$ range of 2.3–10.9 $Å^{-1}$. The inset panel depicts a plot of the calculated average Pr–Fe/Al bond distance and the Debye–Waller coefficient for the Pr coordination sphere relative to the same in the parent compound. These data were deduced from a least-squares fitting of a FF $r$ range indicated by the arrows.

## ACKNOWLEDGMENT

This work was performed in part at the National Synchrotron Light Source at Brookhaven National Laboratory (Upton, NY), which is supported by the U.S. Department of Energy.

[1] J. M. D. Corey and H. Sung, J. Magn. Magn. Mater. **87**, L251 (1990).
[2] H. Sung *et al.*, J. Phys.: Condens. Matter **2**, 6565 (1990).
[3] K. H. J. Buschow *et al.*, J. Magn. Magn. Mater. **92**, L35 (1990).
[4] G. J. Long *et al.*, J. Appl. Phys. **76**, 5383 (1994).
[5] W. B Yelon *et al.*, J. Appl. Phys. **73**, 6029 (1993).
[6] Z. Hu *et al.*, J. Appl. Phys. **76**, 443 (1994).
[7] K. G. Suresh and K. V. S. Rama Rao, in *International Symposium on Magnetic Anisotropy and Coercivity in Rare Earth - Transition Metal Alloys, Sao Paulo, 1996* (World Scientific, Singapore, 1996), p. 391.
[8] K. G. Suresh and K. V. S. Rama Rao, J. Appl. Phys. **79**, 345 (1996).
[9] G. J. Long *et al.*, J. Appl. Phys. **72**, 4845 (1992).
[10] G. J. Long *et al.*, J. Appl. Phys. **74**, 504 (1993).
[11] K. G. Suresh and K. V. S. Rama Rao, J. Less-Common Met. **238**, 90 (1996).
[12] K. G. Suresh and K. V. S. Rama Rao, IEEE Trans. Magn. **31**, 3722 (1995).
[13] K. G. Suresh and K. V. S. Rama Rao, Phys. Rev. B **55**, 15060 (1997).
[14] R. A. Neiser *et al.*, Nucl. Instrum. Methods Phys. Res. A **266**, 220 (1988).
[15] D. C. Koningsberger and R. Prins, *X-ray Absorption: Principles, Applications, Techniques of EXAFS, SEXAFS and XANES,* Vol. 92 (Wiley, New York, 1988).
[16] J. J. Rehr, S. I. Zabinsky, and R. C. Albers, Phys. Rev. Lett. **69**, 3397 (1992).
[17] The NN bond distances are calculated using lattice parameters of $a=8.621$ Å and $c=12.518$ Å.
[18] T. W. Capehart, R. K. Mishra, and F. E. Pinkerton, Appl. Phys. Lett. **58**, 1395 (1991).

[This article is copyrighted as indicated in the article. Reuse of AIP content is subject to the terms at: http://scitation.aip.org/termsconditions. Downloaded to ] IP: 131.193.242.169 On: Thu, 27 Nov 2014 05:08:12